Cr(VI) and Cr(III) Release From Different Layers of Cast Iron Corrosion Scales in Drinking Water Distribution Systems: The Impact of pH, Temperature, Sulfate, and Chloride

Yimei Tian
Tianjin University
Tiantian Yu
Tianjin University
Jingyi Shen
Tianjin University
Guolei Zheng
Tianjin University
Han Li
Tianjin University
weigao zhao (zhaoweigao@outlook.com)
Tianjin University https://orcid.org/0000-0002-4955-1626

Research Article

Keywords: Drinking water distribution systems, Cast iron pipe, Chromium accumulation, Chromium release, Corrosion scales, Iron (oxyhydr)oxides

Posted Date: March 16th, 2021

DOI: https://doi.org/10.21203/rs.3.rs-273416/v1

Abstract

Chromium accumulated from source water and pipeline lining materials in corrosion scales could potentially be released into bulk water in drinking water distribution systems (DWDS). Chromium behaviors between corrosion scale phase and the surrounding water phase vary spatially in different layers and temporally in different DWDS running periods. In this study, corrosion scales sampled from actual DWDS were first characterized by SEM, XRD, XRF, and the modified BCR three-step sequential extraction procedure. Then scales were divided into the outer and inner layers for subsequent analysis. Static accumulation and release experiments were performed with Cr(VI) and Cr(III) on two distinct scale layers to systematically assess the influence of pH, temperature, sulfate, and chloride. The release behaviors of Cr(VI) under the co-effect of multiple factors were investigated in orthogonal experiments. Results showed that in the outer and inner layers of corrosion scales, chromium exhibited differences in accumulation and release behaviors, with the outer layer accumulating less and releasing more. The mechanisms of chromium retention based on different iron (oxyhydr)oxides were discussed.

Highlights

- Chromium speciation and distribution in iron corrosion scale layers were assessed.
- Chromium was more mobile and available in the outer layer than the inner core layer.
- Cr(VI) was more likely to accumulate in iron corrosion scales than Cr(III).
- Outer layers of scales accumulated less and released more chromium than inner layers.
- Factors influencing outer layer Cr(VI) release were temperature sulfate pH chloride.

1. Introduction

Drinking water safety and quality are fundamental to human health and social development. It is estimated that in China the drinking water quality classification in metropolitan areas reduces by about 10% throughout drinking water distribution systems (DWDS). Corrosion scales in pipelines are one of the major factors responsible for this reduction in quality and are a key concern, serving as a source and a sink for various contaminants. Heavy metals can accumulate in corrosion scales and under certain conditions be released into drinking water, significantly reducing water quality (Gerke et al., 2016; Li et al., 2020b; Liu et al., 2019; Peng and Korshin, 2011; Peng et al., 2010). Although the concentration of metallic pollutants in drinking water are generally below the limits specified by guidelines, gradual accumulation and release from corrosion scales can significantly increase concentrations of heavy metals in drinking water, with reportedly reaching ten-fold (Li et al., 2019a; Li et al., 2020b). Subsequently, major health risks and aesthetic issues may occur (Liu et al., 2017; Zhang et al., 2020).

Fe, Ca, Mn, Zn, Al are the dominant metallic pollutants identified in iron corrosion scales (Andra et al., 2014; Gao et al., 2019; Li et al., 2018). However, chromium has also been detected in many scale samples (Liu et al., 2016; Peng et al., 2012; Sun et al., 2017; Tong et al., 2019). In recent years, chromium

contamination in DWDS has attracted increasing attention due to its mobility and toxicity. Source water and leaching from cement mortar linings are the two of the main sources of accumulated chromium in DWDS (Estokova et al., 2018; Veschetti et al., 2010). The toxicity of chromium is largely related to its valence state (Moreira et al., 2018). Long-term exposure to high concentrations of Cr(VI) will pose a severe health risk by adversely affecting the immune system. In contrast, Cr(III) is an essential nutrient at trace levels (Liu and Yu., 2020). According to World Health Organization (WHO) recommendations, the maximum permitted concentration of Cr(VI) in drinking water is 0.05 mg/L (WHO, 2017). However, Cr(III) has the potential to be oxidized into Cr(VI) by strong oxidants such as chlorine, ozone and permanganate, which are commonly used as disinfectants in the water treatment process (Chebeir et al., 2016; Lindsay et al., 2012). As a result of these toxicological risks, environmental conditions that influence the accumulation or release of both Cr(VI) and Cr(III) are of concern.

Water quality parameters such as temperature, pH, alkalinity, sulfate and chloride concentrations, affect interactions between the corrosion scale phase and water phase. (Li et al., 2019a; Li et al., 2019b; Li et al., 2020a; Lytle et al., 2020; Sun et al., 2017; Wang et al., 2019). Heavy metals accumulated in corrosion scales have been found to have different structures and compositions with varying water quality parameters, hydraulic conditions and pipe materials, resulting in different accumulation and release behaviors (Li et al., 2016; Li et al., 2019b; Zhuang et al., 2019). Previous studies on corrosion scales have demonstrated that higher temperatures are typically associated with higher corrosion rates and increased microbiological processes, leading to an increase in heavy metal release (Li et al., 2020a; Zhang et al., 2020). Water pH is also an important influencing factor, as it changes the surface charge of corrosion scales, the speciation distribution and degree of ionization of heavy metals (Li et al., 2016; Zhang et al., 2020). Acidic conditions generally increase Mn and Fe release, resulting in a rise in turbidity and discoloration issues (Liu et al., 2017). Chloride and sulfate have been observed to have relatively complex effects on the release of heavy metals. Some studies have demonstrated that an increase in sulfate and chloride concentrations increases heavy metal release from corrosion scales (Hu et al., 2018; Li et al., 2020b; Peng et al., 2013). While inconsistent results were reported by Lytle et al. (2020), suggesting that the effect of sulfate and chloride on metal release behaviors depend on conditions or multiple factors. Furthermore, Zachara et al. (1988) found that excess sulfate was likely to enhance the sorption of chromium. However, few studies have systematically investigated the influencing factors and mechanisms of chromium accumulation and release from iron corrosion scales, or the behavior of chromium under the co-effect of multifactors.

The composition and structure of corrosion scales can also influence heavy metal accumulation and release behaviors. To date, the characteristics of corrosion scales on different pipe materials, under different conditions, have been analyzed most comprehensively (Liu et al., 2016; Peng et al., 2010; Niu et al., 2006; Sarin et al., 2004). Typical iron corrosion scales are composed of three distinct layers, a surface layer, a shell-like layer, and a porous core layer (Sarin et al., 2001). Different structures and compositions have been observed in samples from different layers of the same corrosion scale tubercle. The formation of corrosion scales is a dynamic process and with ongoing of DWDS, the scale layer thickens and the original outer layer gradually becomes an inner layer. The significant physiochemical difference between

layers may affect heavy metal release. Therefore, the behaviors of heavy metals in corrosion scales may vary spatially, in different corrosion scale layers and temporally, in different DWDS running periods. However, few studies have comprehensively analyzed these differences.

Therefore, in this study, chromium behaviors between corrosion scale phase and the surrounding water phase were investigated spatially in different scale layers. The aim of this work were to: 1) identify the physicochemical distributions of heavy metals in different layers of grey cast iron corrosion scales; 2) reveal the impact of pH, temperature, sulfate and chloride on chromium retention by different scale layers; 3) analyze chromium retention mechanisms based on different iron (oxyhydr)oxides; 4) investigate release behaviors of Cr(VI) under co-effect of multiple factors and provide reference for Cr(VI) control strategies in DWDS.

2. Materials And Methods

2.1 Samplecollection and layering

Corrosion scales were sampled from a 200 mm-diameter gray cast iron pipe that had been in service for more than 20 years in the drinking water distribution system of Tianjin, China (Fig. S1 (a)). Samples were sealed in bottles filled with nitrogen before use. Certain layering characteristics were typically observed in most of iron corrosion scales (Fig. S1(b)). Layering was done with a spatula. The surface layer was a yellowish-brown thin sliding layer of about 0.5 mm, which was directly in contact with bulk water in DWDS. Lightly scraped off the surface layer with a spatula, the middle layer was found of shell-like layer, exhibiting a black, metallic luster, with a relatively hard and dense structure. After scraping off the middle layer, the rest was the porous core layer, which was yellow and black with a relatively loose structure. Prior to all experiments, the layered samples were separately crushed and passed through 100-mesh nylon sieves to ensure samples were fully homogenized. The collected powder samples were then dried in a freeze dryer and stored at 4 ℃ for analysis. The layered samples were partly used for characterization and BCR procedure, and part for the subsequent accumulation and release experiments. For the latter, the surface layer and shell-like layer were combined as the outer layer, while the porous core layer was considered as the inner layer. While it was worth noting that to ensure the uniformity of scales for the accumulation and release experiments, heavy metals contained in the original corrosion scales should be released first. Thus that part of scale blocks were soaked with ultrapure water for 72 h, with ultrapure water replaced every 24 h. The soaked scales were then dried and crushed as mentioned above.

2.2 Characterization of iron corrosion scales

The morphology of three scale layers was observed by scanning electron microscopy (SEM, HITACHI S-4800, Japan). X-ray fluorescence spectrometer (XRF, S4 Pioneer, German) were used to analyze the elemental content of corrosion scale samples. The X-ray diffraction (XRD) spectra were obtained by X-ray diffractometer (XRD, D/MAX-2500, Japan) to identify crystalline solid phases. The concentration of heavy metals in the original corrosion scales were analyzed by inductively coupled plasma mass spectrometry (ICP-MS, Agilent 7700X, USA).

2.3 Modified BCR three-step sequential extraction procedure

The modified BCR three-step sequential extraction procedure was performed to establish the physicochemical speciation distributions of heavy metals in different layers of corrosion scale samples. The experimental procedure is outlined in detail in Table S1 (Rauret et al., 1999), with all extracts then filtered through 0.45 μm membrane filters and stored at 4 ℃ for analysis by ICP-MS.

The modified BCR three-step sequential extraction process partitions elements into four fractions, classified as exchangeable and acid-soluble, reducible, oxidizable, and residual. The exchangeable and acid-soluble fraction is composed of both the exchangeable fraction and carbonate-bound fraction, containing heavy metals associated with exchangeable binding sites and carbonates. Heavy metals in the exchangeable fraction are relatively easily displaced by competing ions. Acid-soluble fraction metals are coprecipitated with calcite and therefore, can be easily dissolved by acid. The reducible fraction was dominated by heavy metals bound to Fe-Mn oxides. pH and oxidation-reduction potential (ORP) in DWDS have a significant influence on the migration and transformation of the reducible fraction. When the water is reducible or anoxic, Fe-Mn oxides tend to dissolve and heavy metals are released. The oxidizable fraction refers to metals bound with complex organics or sulfides, which are easily decomposed and released under oxidation conditions. The residual fraction consists of metals in the form of crystallised oxides within the crystal lattice of minerals, resulting in these metals being stable and non-bioavailable (Linge, 2008). Therefore, in contrast to the residual fraction, the other extractable fractions are relatively highly mobility and active, presenting a significant risk of pollution due to their environmental availability (Barcelos et al., 2020). In this study, the three non-residual fractions were considered together, to assess the mobility and release potential of heavy metals in each layer of corrosion scales under varying conditions.

2.4 Static accumulation and release experiments

Visual MINTEQ 3.1 was used to calculate chromium speciation under different pH conditions. All experiments were conducted with ultrapure water as the background water to eliminate the interference of other ions. For data quality control, each sample was measured in duplicate with results showing an error of less than ± 5.0%.

2.4.1 Accumulation of Cr(III) and Cr(VI)

According to the water quality conditions reported in real DWDS pipelines, the initial pH value and temperature were selected as variable factors in accumulation experiments. Initial concentration of chromium was set as 2.5 mg/L on the basis of relevant water quality standard of WHO, to simulate the rapid accumulation of chromium in pipe network accidents. The accumulation experiments were conducted independently for Cr(III) and Cr(VI), as shown in Table S2. For each pH condition (pH 4, pH 5.5, pH 7, pH 8.5, pH 10), 25 mL of chromium solution was added to a 50mL centrifuge tube that had been soaked in 10% nitric acid solution and rinsed prior to use. The solutions were then placed in a constant temperature shaker at 250 rpm for 1440 min, with 0.00250 g of layered scale powder then added after the

required temperature (5 ℃, 15 ℃, 25 ℃) was reached. In addition, another experimental group was established at 25 ℃ and pH 7 for kinetic analysis, with solution samples collected at 0, 5, 10, 30, 60, 120, 240, 360, 480, 720, 1440, and 2880 min. Following collection, all solution samples were filtered through 0.45 μm membrane filters and acidified with nitric acid to obtain pH < 2 solutions. Inductively coupled plasma emission spectrometry (ICP-OES, THERMO iCAP-7400, USA) was then used to analyze chromium concentration in the solutions.

2.4.2 Release of Cr(III) and Cr(VI)

Release experiments were conducted to assess the influence of variations in key factors of pH, temperature, sulfate, and chloride. The experimental parameters are described in detail in Table S3. The scale powder samples were pretreated by enrichment with 10 mg/L of chromium standard reserve fluid for 24 h. More details can be found in the supplementary material. Centrifuge tubes were removed at 0, 5, 10, 30, 60, 120, 240, 360, 600, 720, 1440, 2880, and 4320 min, for analysis. The remaining experimental steps were the same as accumulation experiments, with ICP-MS used to analyze chromium concentrations.

2.4.3 Orthogonal experiments on Cr(VI) release

Orthogonal experiments were performed to identify the significance of factors affecting Cr(VI) release from different layers of iron corrosion scales. pH, temperature, sulfate, and chloride were applied as experimental factors, with each factor having three variation levels. The orthogonal design table L_9 (4^3) is shown in Table S4. All of the 9 experimental trials were carried out in parallel duplicate experiments. The Cr(VI) concentration in solution was measured at 2880 min. Range analysis was conducted to assess and compare the influencing degree of all four factors. The corresponding average k_i value and R value were calculated. The k_i value represents the impact of the three variation levels of each factor, which was calculated as the mean concentration of Cr(VI) released. The R value indicates the difference between the maximum and minimum k_i value for the three variation levels for each factor, with the factor exhibiting the highest R value having a stronger impact on Cr(VI) release. Variance analysis was also performed using SPSS v.22.0 to assess the significance of each factor.

3. Results And Discussion

3.1 Characterization and speciation distribution of each scale layer

SEM images (Fig. 1) have demonstrated the differences in morphology of each scale layers. More loose and porous structure could be observed in the porous core layer (Fig. 1 (c)), which may be beneficial for metal adsorption and accumulation. More significant characteristics can be seen from images magnified by 50,000 times (Fig. 1 (d), (e), and (f)). Combined with the XRD spectra result (Fig. S2), the main components defined in the shell-like layer of the corrosion scales were magnetite (Fe_3O_4) and hematite (Fe_2O_3), considered to be relatively stable. Goethite (a-FeOOH) and lepidocrocite (γ-FeOOH) were the main

crystalline iron minerals in surface layer and porous core layer. Table S5 and S6 shows the distribution of metal content in different layers of the iron corrosion scales. Cr exhibited the highest content in the surface layer of 102.63 mg/kg. And the contents of Cr in the shell-like layer and the porous core layer were 37.67 mg/kg and 47.05 mg/kg, which showed little difference. The total content of Cr was 187.35 mg/kg, that was comparable to the 90th percentile level in Peng's study of 58 scale samples from 20 US drinking water utilities (Peng et al., 2012).

The speciation distribution of metal elements in each scale layer was investigated to analyze their mobility and release potential in corrosion scales (Figure 2). The fraction distribution of Fe showed little difference in each of the three layers. But beyond that, the residual fraction of all the other metal elements was significantly much more in the porous core layer, especially for Al (83.46%) and Cr (72.05%). This result demonstrates that metal elements in the porous core layer mainly present in stable matrices and were relatively immobile. Whereas metal elements in the surface layer and shell-like layer have stronger mobility and release potential. Therefore, the surface layer and shell-like layer of corrosion scale samples were combined to represent the outer layer in subsequent studies, in comparison to the inner porous core layer. In the surface layer and shell-like layer, the majority of Cr (67.34% and 41.78%) existed in reducible fraction. This corroborated that the reducible fraction dominated by heavy metals bound to Fe-Mn oxides exhibited a strong affinity for Cr (Rai et al., 1989).

3.2 Factors influencing chromium accumulation

3.2.1 Effect of pH

The effects of pH on chromium accumulation are shown in Fig. 3 (a). Data was measured at 1440 min when the accumulation process was approaching chemical equilibrium. Results demonstrated that the accumulated amount of Cr(VI) slightly increased under higher pH conditions, and the average value was about 1.6 mg/L. But it is of note that Cr(III) accumulation was much smaller than Cr(VI) and changed dramatically when pH increased to 10. Previous studies have shown that under acidic conditions, H^+ ions and metal ions compete with each other for the available surface sites (Gu et al., 2018), resulting in less heavy metal accumulation in corrosion scales. In addition, pH affects chromium speciation, especially Cr(III). The simulation results by Visual MINTEQ 3.1 (Fig. S3 (b)) show that Cr^{3+} and $Cr(OH)^{2+}$ were the dominant species under acidic conditions, while under neutral conditions, Cr(III) mainly existed in the form of $Cr(OH)_3$ precipitation. At pH levels above 10, Cr(III) existed partially in the form of $Cr(OH)_4^-$. Therefore, although the initial concentration of Cr(III) was 2.5 mg/L, the actual concentrations present in solution were 1.83, 1.7, 0.23, 0.32, 1.66 mg/L at pH 4, pH 5.5, pH 7, pH 8.5, pH 10, respectively. Thus the accumulation ratio was calculated and illustrated in Fig.S4 (a). Similarly, Cr(VI) accumulation ratio increased slightly as pH rose. The accumulation ratio of Cr(III) showed a rising trend in general but increased rapidly around pH 7. This was mainly attributed to the high level of $Cr(OH)_3$ precipitation under near-neutral pH conditions. The accumulation ratio of Cr(VI) was about 90 % under all experimental pH conditions, significantly higher than that of Cr(III).

However, the pH of water in DWDS is universally neutral and at pH 7 the average amount of Cr(VI) accumulated was 1.56 mg/g. While only 0.16 mg/g Cr(III) was found to accumulate on average, approximately ten-fold less than Cr(VI) under the same pH conditions. There was also a difference of about 20% in accumulation ratio. This indicated that in DWDS Cr(VI) release should be considered as a major concern, due to its high toxicity and potential for accumulation.

3.2.2 Effect of temperature

The effect of temperature on chromium accumulation was investigated at different temperature conditions of 5 ℃, 15 ℃, and 25 ℃. Temperature mainly exerts an influence by affecting the reaction rate, chemical equilibrium and microbiological processes. Fig. 3 (b) and Fig. S4 (b) shows the result. The mean accumulated amounts of Cr(VI) were 2.24, 2.25, and 2.10 mg/g at temperatures of 5 ℃, 15 ℃, and 25 ℃, respectively, indicating that temperature exerted no significant effect on Cr(VI) accumulation. For Cr(III), rising temperatures induced an increase in accumulation, with the ionic mobility of chromium increasing, resulting in a greater contact probability between chromium and available sites on the corrosion scale surface (Gupta et al., 2013). When the temperature was 25 ℃, the accumulated amount and ratio of Cr(III) both reached a maximum level of 0.016 mg/g and about 70 % on average. Overall, Cr(VI) accumulation in corrosion scales was much greater than Cr(III) accumulation.

On the other hand, chromium accumulated in the inner layer was always more than that in the outer layer in general. Moreover, the accumulation of Cr(VI) was significantly greater than that of Cr(III). Compared with Cr(III), results indicate that it is easier for Cr(VI) to migrate from the water phase to the corrosion scale phase and, thus Cr(VI) was more likely to be absorbed and accumulate in corrosion scales.

3.2.3 Cr (VI) accumulation kinetics

The effects of reaction time on Cr(VI) accumulation are shown in Fig. S5. Due to sufficient availability of surface sites, the accumulation rate of Cr(VI) increased rapidly within the initial 60 min. However, equilibrium was not reached until 2880 min. To further investigate the mechanisms of Cr(VI) accumulation, the pseudo-first-order kinetic model, pseudo-second-order kinetic model, Elovich model, and Webber Morris intra-particle diffusion model were used to analyze Cr(VI) accumulation kinetics data. The kinetic parameters of these four models are summarized in Table S7. The correlation coefficients (R^2) of the pseudo-second-order kinetic model were greater than that of the pseudo-first-order kinetic model, indicating that the rate-limiting step was the chemisorption process. The Elovich model R^2 values for outer layer and inner layer Cr (VI) accumulation were 0.889 and 0.910, respectively. The validity of the Elovich model implies that the initial Cr (VI) accumulation process was rapid, while the desorption process was slow and occasional (Labied et al., 2018). Webber-Morris intra-particle diffusion model data exhibited two unique linear plots, demonstrating that the accumulation procedure was not only controlled by intraparticle diffusion.

3.3 Factors influencing chromium release

3.3.1 Effect of pH

Similar to the accumulation process, pH affected chromium release by changing the surface charge and degree of ionization of corrosion scales, the speciation distribution of chromium. Under low pH conditions, Cr(VI) mainly exists in the forms of $HCrO_4^-$, while CrO_4^{2-} is the dominant species under high pH conditions. CrO_4^{2-} can easily bind with heavy metals in corrosion scales (Xu et al., 2011). The effect of pH on Cr(VI) release is shown in Fig. 4. The Cr(VI) equilibrium release amounts in the outer layer and the inner layer were both ranked in the descending order of pH 4 > pH 7 > pH 5.5 > pH 10 > pH 8.5. Overall, acidic conditions were beneficial to Cr(VI) release, while alkaline conditions impeded release. With a reduction in pH, ion-exchange processes occur between H^+ ions and Cr(VI) ions (Jin et al., 2018). Meanwhile, H^+ ions promote the dissolution of Fe-Mn oxides (Guo et al., 2019), increasing Cr(VI) release from corrosion scales. Furthermore, an increase in pH may convert aqueous chromium ions into hydrolyzed ion forms, resulting in lower solvation energies being required for the surface binding process (Moutsatsou et al., 2006). However, Cr(VI) release reached a minimum level at pH 8.5 rather than pH 10, which may partly be due to higher pH conditions resulting in excessive deprotonation of the corrosion scale surface, decreasing the affinity between CrO_4^{2-} ions and corrosion scales (Rahman et al., 2013).

Under all pH conditions tested, Cr(VI) released from the outer layer of corrosion scales was consistently greater than from the inner layer, which could be explained by different physicochemical speciation distributions of chromium, as shown in Fig. 2. The results of sequential extraction show that chromium in the outer layer of corrosion scales possessed greater mobility than the inner layer. In addition, chromium mainly existed in a bound form with carbonate minerals and Fe-Mn oxides in the outer layer, exhibiting to be more sensitive to pH variations.

Compared with Cr(VI), the release of Cr(III) fluctuated considerably, as shown in Fig.4 (c) and (d). This was largely due to the release amount of Cr(III) being much smaller and therefore, more affected by instrument error. Results appear to show that Cr(III) has weaker mobility and was less easily released from the corrosion scale phase to the water phase.

3.3.2 Effect of temperature and release kinetics

In general, DWDS temperature conditions exhibit distinct seasonal and diurnal changes. Therefore, the effects of temperature on chromium release were studied and the results are shown in Fig. 5. The amount of Cr(VI) released at 25 ℃ (28.10 μg/L from the outer layer, 23.82 μg/L from the inner layer) was significantly greater than at 5 ℃ (10.35 μg/L from the outer layer, 10.22 μg/L from the inner layer) or 15 ℃ (13.81 μg/L from the outer layer, 12.76 μg/L from the inner layer). This may be attributed to the mobility of metal ions and the ion exchange rate being increased at higher temperatures, thereby chromium migrated more easily from the corrosion scale phase to the water phase. Moreover, the increase in temperature could accelerate the dissolution of precipitants such as carbonate bound fractions, resulting in an increase in the release of chromium.

Cr(VI) release kinetics tests in the temperature range of 5 ℃ to 25 ℃ were performed to further illustrate the effect of temperature, with the Elovich model, Double constant model, and pseudo-second-order kinetic model applied. Detailed information and parameters for these models are provided in Table S8. The kinetic models selected all fitted data well (Fig. 5 (a)), while the Elovich model fitted best on the whole, indicating that chromium release may be controlled by a variety of complex reaction mechanisms.

The values of the parameters for the two-constant model at different reaction temperatures (Table S8) showed that the values of the initial release rate constant 'a_2' varied relatively widely. This is consistent with previous results on the increase of Cr(VI) release as temperature went higher. In Elovich model, value 'a_1' represents the initial desorption rate and value 'b_1' is the desorption constant (Rezaei Rashti et al., 2014). In the present study, the Elovich model rate constant 'a_1' values increased widely in both the outer layer and the inner layer when temperature increased (Table S7). Moreover, the values of constant 'b_1' were compared in the outer layer and the inner layer, showing that 'b_1' values in the outer layer were consistently larger at all assessed temperatures. This result is can also be explained by the different physicochemical speciation distributions of chromium in the two iron corrosion scale layers.

The release of Cr(III) under all conditions was less than 8 μg/L, with data showing no obvious trend with varying temperature conditions (Fig. S6). However, combined with the data on the effects of temperature on Cr(VI) release, it can be concluded that the release potential of chromium is theoretically smaller at lower temperatures. Therefore, more attention should be paid to chromium release in high temperature environments and seasons.

3.3.3 Effect of sulfate and chloride

The concentration of chromium released into solution under three sulfate and chloride concentrations (50, 150, 250 mg/L) was determined over time. Fig. 6 (a) and (b) exhibit the effect of sulfate on Cr(VI) release. In the outer layer, the equilibrium concentrations of Cr(VI) in solution were 47.52, 69.13 and 31.64 μg/L at sulfate concentrations of 50, 150, and 250 mg/L, respectively. The data for Cr(VI) release from the inner layer showed a similar trend with 22.23, 27.52 and 18.16 μg/L, although with relatively less variation. This could be attributed to competitive adsorption and competitive electron transfer reactions occurring between chromium ions and sulfate (Meena and Arai, 2016). Furthermore, sulfate may affect the structure, solubility, or microbiological processes in corrosion scales (Lytle et al., 2020), resulting in sulfate being beneficial to chromium release. However, when the concentration of sulfate increased to 250 mg/L, Cr(VI) release decreased. It has previously been reported, that excess sulfate appears to increase the sorption of chromium (Zachara et al. 1988). A possible explanation for this may be that complexes are formed between sulfate and Cr(VI), resulting in re-absorption onto corrosion scales. It has previously been demonstrated that a new species $CrO_3SO_4^{2-}$ was formed in the presence of sulfate (Han et al., 2008).

The effect of chloride on Cr(VI) release is presented in Fig. 6 (c) and (d). When the concentration of chloride increased from 50 mg/L to 150 mg/L, the equilibrium concentration of released Cr(VI) increased

from 8.94 to 13.20 μg/L, respectively. Similarly to sulfate, chloride also competes with heavy metals for adsorption sites and electron transfer reactions (Peng et al., 2013), increasing Cr(VI) release. The presence of sulfate and chloride could also increase the acidity of the solution (Sarin et al., 2004), promoting the dissolution of iron corrosion scales. However, when the concentration of chloride was increased to 250 mg/L, chromium release decreased by about 4.24 μg/L compared with that at 150 mg/L chloride, which was in agreement with previously reported results (Lytle et al., 2020). This phenomenon may occur due to the existence of CrO_3Cl^- under excessive chloride concentrations (Han et al., 2008), indicating that chloride may complex with Cr(VI) and therefore inhibit Cr(VI) release.

Fig. S7 illustrates the effects of varying concentrations of sulfate and chloride on Cr(III) release. The effect of sulfate on Cr(III) release was similar to the effect on Cr(VI), while chloride exerted no significant effect. However, the level of Cr(III) release was less than 5 μg/L and therefore, values fluctuated greatly and were more affected by instrument measurement error. Overall, sulfate and chloride exerted a similar effect on chromium release. When the concentration of sulfate or chloride increased from 50 mg/L to 150 mg/L, an increase in chromium release was observed. In contrast, an excess of sulfate or chloride (250 mg/L) may result in the formation of complexes with chromium ions, resulting in the inhibition of chromium release.

3.4 Analysis of factors affecting Cr(VI) release according to the results of the orthogonal experiments

Fig. 7 shows the results of orthogonal experiments based on range analysis. Detailed data is presented in Table S9 and Table S10. Results demonstrate that Cr(VI) released from the outer and inner layer exhibited similar trends under the co-effect of multifactors. Whereas Cr(VI) released from the inner layer was always less than that from the outer layer, which also illustrates the significant difference in heavy metal release from different layers of corrosion scales. As for the outer layer, temperature, sulfate, pH, and chloride exerted an inhibitory effect on Cr(VI) release (in descending order), as shown by the range analysis calculation results. According to the results of variance analysis (Table S11), temperature, sulfate, and pH had significant effects (1% significance level) on Cr(VI) release. Meanwhile, chloride was found to have a significant effect (5% significance level). Based on the results of this study, during the stable running period of DWDS, lower temperatures, alkaline pH values, and lower concentrations of sulfate and chloride can have significant effects on controlling Cr(VI) release. However, temperature is typically an uncontrolled factor in DWDS, hence the monitoring of water quality in DWDS should be strengthened in high temperature seasons and locations, to prevent rapid and large-scale release of heavy metals in drinking water resources. Furthermore, only modest changes are observed in the pH values in DWDS. Subsequently, the concentrations of sulfate and chloride in DWDS should be the main focus in control strategies, especially sulfate.

As for the inner layer, according to the range analysis and variance analysis, pH exerted a significant effect on Cr(VI) release at the 5% significance level, while temperature exerted a significant effect at the 10% level. In contrast, sulfate and chloride exerted no significant effect on Cr(VI) release. Similar to the

results for the outer layer, control strategies should focus on the occurrence of heavy metal release due to seasonal changes in water temperature.

3.5 Mechanism analysis

Combined all the results, it could be concluded that the behaviors of chromium differed in corrosion scales, spatially in different layers and temporally in different DWDS running periods. The complexity of corrosion scales and DWDS makes it difficult to determine the mechanism. Some studies have investigated that surface complexation, surface precipitation are the principal mechanisms of chromium retention by iron (oxyhydr)oxides (Johnston and Chrysochoou, 2014; Kumar et al., 2014; Shi et al., 2021). Surface precipitation of $Cr(OH)_3$ is the main retention mechanism of Cr(III) at neutral pH conditions. For Cr(VI), the initial driving force might be the electrostatic attraction between positively charged iron (oxyhydr)oxides and negatively charged Cr(VI) species (Fischer et al., 2007). Then ion exchange between surface hydroxyl and chromium is the principal mechanism involved (Zhang et al., 2019). Inner-sphere complexation may form through ligand exchange, while electrostatic interaction or van der Waals forces count on outer-sphere complexation (Kumar et al., 2014). Mineral species, metal species, and reacting conditions all make a difference to specific process. Section 3.1 have analyzed the difference in mineral composition of each scale layer. The shell-like layer was mainly composed of more thermodynamically stable iron oxides (hematite (Fe_2O_3) and magnetite (Fe_3O_4)). Whereas surface layer and porous core layer were dominated by iron oxyhydroxides (goethite (a-FeOOH) and lepidocrocite (γ-FeOOH)), relatively instable. The differences in crystallographic face and bulk structure of iron (oxyhydr)oxides make the retention mechanism and metal capacity vary. The mechanism analysis diagram of chromium retention by iron (oxyhydr)oxides is shown in Fig.S8.

Goethite (a-FeOOH) and lepidocrocite (γ-FeOOH) are different crystal forms of iron oxyhydroxide. Lepidocrocite (γ-FeOOH) has layered structure and goethite (a-FeOOH) has tunnel structure. CrO_4^{2-} has a strong affinity on goethite (a-FeOOH) surface, especially under acidic conditions. Similar to hematite (Fe_2O_3), the dominant species changed from diodentate complex to monulnar complex with the increase of pH (Marchi et al., 2015). Wu et al. shows that lepidocrocite (γ-FeOOH) exerted higher Cr(VI) removal efficiency than goethite (a-FeOOH) (Wu et al., 2016).

Hematite (Fe_2O_3) is rhombohedral hexagonal and isomorphic to corundum. Several studies have suggested that the retention mechanism and chromium capacities of hematite (Fe_2O_3) were independent of ionic strength, but closely related to pH values (Johnston and Chrysochoou, 2012, 2014; Huang et al., 2016). Johnston and Chrysochoou revealed that nonprotonated monodentate complexes were dominant at pH 6 and above while more bidentate complexes were found below pH 6 (Johnston and Chrysochoou, 2014).

The crystallographic form of magnetite (Fe_3O_4) is cubic inverse spinel (Shi et al., 2021), the existence of both Fe^{2+} and Fe^{3+} in its structure make it different from other iron (oxyhydr)oxides. Oxidation–reduction

between Cr(VI) and magnetite (Fe_3O_4) provides another mechanism for Cr(VI) retention (Chowdhury et al., 2012).

4. Conclusions

The mobility and toxicity of chromium is largely dependent on their physicochemical speciation. For the first time, the accumulation and release behaviors of chromium were assessed in two distinct layers of iron corrosion scales based on the speciation distributions of heavy metals. The following conclusions can be reached.

1. The results of modified BCR three-step sequential extraction showed that most of the heavy metals in the surface layer and shell-like layer of iron corrosion scales existed in mobile and bioavailable states.
2. In general, the accumulation of chromium in iron corrosion scales increased under conditions of higher pH and higher temperature. Cr(III) was more sensitive to the variation of pH and temperature, while the accumulated amount of Cr(VI) was significantly greater than that of Cr(III). Neutral or weakly alkaline pH conditions, lower temperatures, and lower concentrations of sulfate and chloride, were found to reduce chromium release. Overall, chromium was found to accumulate more easily in the inner layer, with greater potential to release from the outer layer of iron corrosion scales. Thereinto, Cr(VI) has much more stronger potential of accumulation and release in corrosion scales thus exhibits more health risk.
3. The release behaviors of Cr(VI) under the co-effect of multifactors were demonstrated by orthogonal experiments. Results illustrate that temperature, sulfate, and pH significantly affected Cr(VI) release from the outer layer (1% significance level), followed by chloride (5% significance level). The degree of influence of the four factors on Cr(VI) release from the inner layer was ranked in the descending order of pH temperature chloride sulfate, with chloride and sulfate exerting no significant effect, while pH and temperature had significant effects at the 5% and 10% significance levels, respectively.
4. The surface layer and shell-like layer have similar speciation distribution of metal elements but significantly different crystal structure. The difference of chromium behaviors between the outer and inner layer implies that chromium retention is effected by both metal migration potential and scale crystal structure. Surface complexation, surface precipitation are the principal mechanisms of chromium retention by iron (oxyhydr)oxides.

These findings contribute to both scientific and practical significance in the comprehensive and systematic understanding of chromium behaviors between the corrosion scale phase of two distinct layers and water phase However, this research only considered the accumulation and release behaviors of Cr(VI) and Cr(III) independently, while the influence of co-existing Cr(VI) and Cr(III) and the potential for mutual conversion still requires further investigation.

Declarations

Ethics approval and consent to participate Not applicable

Consent for publication Not applicable

Availability of data and materials The datasets used and/or analysed during the current study are available from the corresponding author on reasonable request.

Competing interests The authors declare that they have no conflict of interest.

Funding This work was supported by the National Natural Science Foundation of China (51778409).

Authors' contributions Yimei Tian: Conceptualization, Supervision, Investigation, Funding acquisition; Tiantian Yu: Methodology, Writing – Review & Editing, Writing-Original Draft; Jingyi Shen: Methodology, Resources, Data Curation; Guolei Zheng: Resources, Data Curation; Han Li: Methodology, Resources; Weigao Zhao: Conceptualization, Investigation, Writing-Original Draft, Validation, Writing – Review & Editing.

References

1. Andra SS, Makris KC, Charisiadis P, Costa CN (2014) Co-occurrence profiles of trace elements in potable water systems: a case study. Environ Monit Assess 186:7307-7320 doi:10.1007/s10661-014-3928-x
2. Barcelos DA, Pontes FVM, da Silva F, Castro DC, Dos Anjos NOA, Castilhos ZC (2020) Gold mining tailing: Environmental availability of metals and human health risk assessment. J Hazard Mater 397:122721 doi:10.1016/j.jhazmat.2020.122721
3. Chebeir M, Chen G, Liu H (2016) Emerging investigators series: frontier review: occurrence and speciation of chromium in drinking water distribution systems. Environ Sci-Wat Res Technol 2:906-914 doi:10.1039/c6ew00214e
4. Chowdhury SR, Yanful EK, Pratt AR (2012) Chemical states in XPS and Raman analysis during removal of Cr(VI) from contaminated water by mixed maghemite-magnetite nanoparticles. J Hazard Mater 235:246-256 doi:10.1016/j.jhazmat.2012.07.054
5. Estokova A, Palascakova L, Kanuchova M (2018) Study on Cr(VI) Leaching from Cement and Cement Composites. Int J Environ Res Public Health 15 doi:10.3390/ijerph15040824
6. Fischer L, Bruemmer GW, Barrow NJ (2007) Observations and modelling of the reactions of 10 metals with goethite: adsorption and diffusion processes. Eur Journal of Soil Science 58:1304-1315 doi:10.1111/j.1365-2389.2007.00924.x
7. Gao J, Liu Q, Song L, Shi B (2019) Risk assessment of heavy metals in pipe scales and loose deposits formed in drinking water distribution systems. Sci Total Environ 652:1387-1395 doi:10.1016/j.scitotenv.2018.10.347
8. Gerke TL, Little BJ, Maynard JB (2016) Manganese deposition in drinking water distribution systems. Sci Total Environ 541:184-193 doi:10.1016/j.scitotenv.2015.09.054

9. Gu F, Zhang Y, Tang Q, Lu C, Zhou T (2018) Remediation of Zn(II)- and Cu(II)-Contaminated Soil Using Citric Acid and Citric Acid-Containing Wastewater. Int J Civ Eng 16:1607-1619 doi:10.1007/s40999-018-0300-5
10. Gupta VK, Pathania D, Agarwal S, Sharma S (2013) Removal of Cr(VI) onto Ficus carica biosorbent from water. Environ Sci Pollut Res 20:2632-2644 doi:10.1007/s11356-012-1176-6
11. Han X, Wong YS, Wong MH, Tam NFY (2008) Effects of anion species and concentration on the removal of Cr(VI) by a microalgal isolate, Chlorella miniata. J Hazard Mater 158:615-620 doi:10.1016/j.jhazmat.2008.02.024
12. Hu J, Dong H, Xu Q, Ling W, Qu J, Qiang Z (2018) Impacts of water quality on the corrosion of cast iron pipes for water distribution and proposed source water switch strategy. Water Res 129:428-435 doi:10.1016/j.watres.2017.10.065
13. Huang X, Hou X, Song F, Zhao J, Zhang L (2016) Facet-Dependent Cr(VI) Adsorption of Hematite Nanocrystals. Environ Sci Technol 50:1964-1972 doi:10.1021/acs.est.5b05111
14. Jin XY, Liu Y, Tan J, Owens G, Chen ZL (2018) Removal of Cr(VI) from aqueous solutions via reduction and absorption by green synthesized iron nanoparticles. J Clean Prod 176:929-936 doi:10.1016/j.jclepro.2017.12.026
15. Johnston CP, Chrysochoou M (2012) Investigation of Chromate Coordination on Ferrihydrite by in Situ ATR-FTIR Spectroscopy and Theoretical Frequency Calculations. Environ Sci Technol 46:5851-5858 doi:10.1021/es300660r
16. Johnston CP, Chrysochoou M (2014) Mechanisms of chromate adsorption on hematite. Geochimica Et Cosmochimica Acta 138:146-157 doi:10.1016/j.gca.2014.04.030
17. Kumar E, Bhatnagar A, Hogland W, Marques M, Sillanpaa M (2014) Interaction of inorganic anions with iron-mineral adsorbents in aqueous media - A review. Adv Colloid Interface Sci 203:11-21 doi:10.1016/j.cis.2013.10.026
18. Labied R, Benturki O, Hamitouche AYE, Donnot A (2018) Adsorption of hexavalent chromium by activated carbon obtained from a waste lignocellulosic material (Ziziphus jujuba cores): Kinetic, equilibrium, and thermodynamic study. Adsorpt Sci Technol 36:1066-1099 doi:10.1177/0263617417750739
19. Li G, Ma X, Chen R, Yu Y, Tao H, Shi B (2019a) Field studies of manganese deposition and release in drinking water distribution systems: Insight into deposit control. Water Res 163 doi:10.1016/j.watres.2019.114897
20. Li M, Liu Z, Chen Y (2018) Physico-chemical Characteristics of Corrosion Scales from Different Pipes in Drinking Water Distribution Systems. Water 10 doi:10.3390/w10070931
21. Li M, Liu Z, Chen Y, Hai Y (2016) Characteristics of iron corrosion scales and water quality variations in drinking water distribution systems of different pipe materials. Water Res 106:593-603 doi:10.1016/j.watres.2016.10.044
22. Li M, Liu Z, Chen Y, Korshin GV (2020a) Effects of varying temperatures and alkalinities on the corrosion and heavy metal release from low-lead galvanized steel. Environ Sci Pollut Res Int 27:2412-

2422 doi:10.1007/s11356-019-06893-2

23. Li M, Liu Z, Chen Y, Zhang M (2019b) Identifying effects of pipe material, hydraulic condition, and water composition on elemental accumulation in pipe corrosion scales. Environ Sci Pollut Res 26:19906-19914 doi:10.1007/s11356-019-05401-w
24. Li M, Wang Y, Liu Z, Sha Y, Korshin GV, Chen Y (2020b) Metal-release potential from iron corrosion scales under stagnant and active flow, and varying water quality conditions. Water Res 175:115675 doi:10.1016/j.watres.2020.115675
25. Lindsay DR, Farley KJ, Carbonaro RF (2012) Oxidation of Cr(III) to Cr(VI) during chlorination of drinking water. J Environ Monit 14:1789-1797 doi:10.1039/c2em00012a
26. Linge KL (2008) Methods for investigating trace element binding in sediments. Crit Rev Environ Sci Technol 38:165-196 doi:10.1080/10643380601174780
27. Liu G et al. (2017) Hotspots for selected metal elements and microbes accumulation and the corresponding water quality deterioration potential in an unchlorinated drinking water distribution system. Water Res 124:435-445 doi:10.1016/j.watres.2017.08.002
28. Liu H, Yu X (2020) Hexavalent chromium in drinking water: Chemistry, challenges and future outlook on Sn(II)- and photocatalyst-based treatment. Fron of Environ Sci Eng 14 doi:10.1007/s11783-020-1267-4
29. Liu J et al. (2016) The spatial distribution of pollutants in pipe-scale of large-diameter pipelines in a drinking water distribution system. J Hazard Mater 317:27-35 doi:10.1016/j.jhazmat.2016.05.048
30. Liu Q, Gao J, Li G, Tao H, Shi B (2019) Accumulation and re-release of metallic pollutants during drinking water distribution and health risk assessment. Environ Sci-Wat Res Technol 5:1371-1379 doi:10.1039/c9ew00291j
31. Lytle DA, Tang M, Francis AT, O'Donnell AJ, Newton JL (2020) The effect of chloride, sulfate and dissolved inorganic carbon on iron release from cast iron. Water Res 183:116037-116037 doi:10.1016/j.watres.2020.116037
32. Marchi G, Vilar CC, O'Connor G, de Oliveira LM, Reatto A, Rein TA (2015) Surface complexation modeling in variable charge soils: Prediction of cadmium adsorption. Revista Brasileira De Ciencia Do Solo 39:1395-1405 doi:10.1590/01000683rbcs20140529
33. Meena AH, Arai Y (2016) Effects of common groundwater ions on chromate removal by magnetite: importance of chromate adsorption. Geochem Trans 17:1 doi:10.1186/s12932-016-0033-9
34. Moreira LJD, da Silva EB, Fontes MPF, Liu X, Ma LQ (2018) Speciation, bioaccessibility and potential risk of chromium in Amazon forest soils. Environ Pollut 239:384-391 doi:10.1016/j.envpol.2018.04.025
35. Moutsatsou A, Gregou M, Matsas D, Protonotarios V (2006) Washing as a remediation technology applicable in soils heavily polluted by mining-metallurgical activities. Chemosphere 63:1632-1640 doi:10.1016/j.chemosphere.2005.10.015
36. Niu ZB, Wang Y, Zhang XJ, He WJ, Han HD, Yin PJ (2006) Iron stability in drinking water distribution systems in a city of China. J Environ Sci 18:40-46

37. Peng C-Y, Ferguson JF, Korshin GV (2013) Effects of chloride, sulfate and natural organic matter (NOM) on the accumulation and release of trace-level inorganic contaminants from corroding iron. Water Res 47:5257-5269 doi:10.1016/j.watres.2013.06.004
38. Peng CY et al. (2012) Occurrence of trace inorganic contaminants in drinking water distribution systems. J Am Water Work Assoc 104:53-54 doi:10.5942/jawwa.2012.104.0042
39. Peng CY, Korshin GV, Valentine RL, Hill AS, Friedman MJ, Reiber SH (2010) Characterization of elemental and structural composition of corrosion scales and deposits formed in drinking water distribution systems. Water Res 44:4570-4580 doi:10.1016/j.watres.2010.05.043
40. Rahman MS, Whalen M, Gagnon GA (2013) Adsorption of dissolved organic matter (DOM) onto the synthetic iron pipe corrosion scales (goethite and magnetite): Effect of pH. Chem Eng J 234:149-157 doi:10.1016/j.cej.2013.08.077
41. Rai D, Eary LE, Zachara JM (1989) Environmental chemistry of chromium. The Sci of the total environ 86:15-23 doi:10.1016/0048-9697(89)90189-7
42. Rauret G, Lopez-Sanchez JF, Sahuquillo A, Rubio R, Davidson C, Ure A, Quevauviller P (1999) Improvement of the BCR three step sequential extraction procedure prior to the certification of new sediment and soil reference materials. J Environ Monit 1:57-61 doi:10.1039/a807854h
43. Rezaei Rashti M, Esfandbod M, Adhami E, Srivastava P (2014) Cadmium desorption behaviour in selected sub-tropical soils: Effects of soil properties. J Geochem Explor 144:230-236 doi:10.1016/j.gexplo.2014.01.023
44. Sarin P, Snoeyink VL, Bebee J, Jim KK, Beckett MA, Kriven WM, Clement JA (2004) Iron release from corroded iron pipes in drinking water distribution systems: effect of dissolved oxygen. Water Res 38:1259-1269 doi:10.1016/j.watres.2003.11.022
45. Sarin P, Snoeyink VL, Bebee J, Kriven WM, Clement JA (2001) Physico-chemical characteristics of corrosion scales in old iron pipes. Water Res 35:2961-2969 doi:10.1016/s0043-1354(00)00591-1
46. Shi M et al. (2021) Recent progress in understanding the mechanism of heavy metals retention by iron (oxyhydr)oxides. Sci Total Environ 752 doi:10.1016/j.scitotenv.2020.141930
47. Sun H, Shi B, Yang F, Wang D (2017) Effects of sulfate on heavy metal release from iron corrosion scales in drinking water distribution system. Water Res 114:69-77 doi:10.1016/j.watres.2017.02.021
48. Tong H, Li Z, Hu X, Xu W, Li Z (2019) Metals in Occluded Water: A New Perspective for Pollution in Drinking Water Distribution Systems. Int J Environ Res Public Health 16 doi:10.3390/ijerph16162849
49. Veschetti E, Achene L, Ferretti E, Lucentini L, Citti G, Ottaviani M (2010) Migration of trace metals in Italian drinking waters from distribution networks. Toxicol Environ Chem 92:521-535 doi:10.1080/02772240903036139
50. Wang J, Yan H, Xin K, Tao T (2019) Iron stability on the inner wall of prepared polyethylene drinking pipe: Effects of multi-water quality factors. Sci Total Environ 658:1006-1012 doi:10.1016/j.scitotenv.2018.12.127
51. Wu S, Lu J, Ding Z, Li N, Fu F, Tang B (2016) Cr(VI) removal by mesoporous FeOOH polymorphs: performance and mechanism. Rsc Advances 6:82118-82130 doi:10.1039/c6ra14522a

52. Xu Y-j, Arrigo R, Liu X, Su D-s (2011) Characterization and use of functionalized carbon nanotubes for the adsorption of heavy metal anions. New Carbon Mater 26:57-62 doi:10.1016/s1872-5805(11)60066-8
53. Zhang L, Fu F, Tang B (2019) Adsorption and redox conversion behaviors of Cr(VI) on goethite/carbon microspheres and akaganeite/carbon microspheres composites. Chem Eng J 356:151-160 doi:10.1016/j.cej.2018.08.224
54. Zhang S, Tian Y, Guo Y, Shan J, Liu R (2020) Manganese release from corrosion products of cast iron pipes in drinking water distribution systems: Effect of water temperature, pH, alkalinity, SO4(2-) concentration and disinfectants. Chemosphere 262:127904 doi:10.1016/j.chemosphere.2020.127904
55. Zhuang Y, Han B, Chen R, Shi B (2019) Structural transformation and potential toxicity of iron-based deposits in drinking water distribution systems. Water Res 165:114999 doi:10.1016/j.watres.2019.114999

Figures

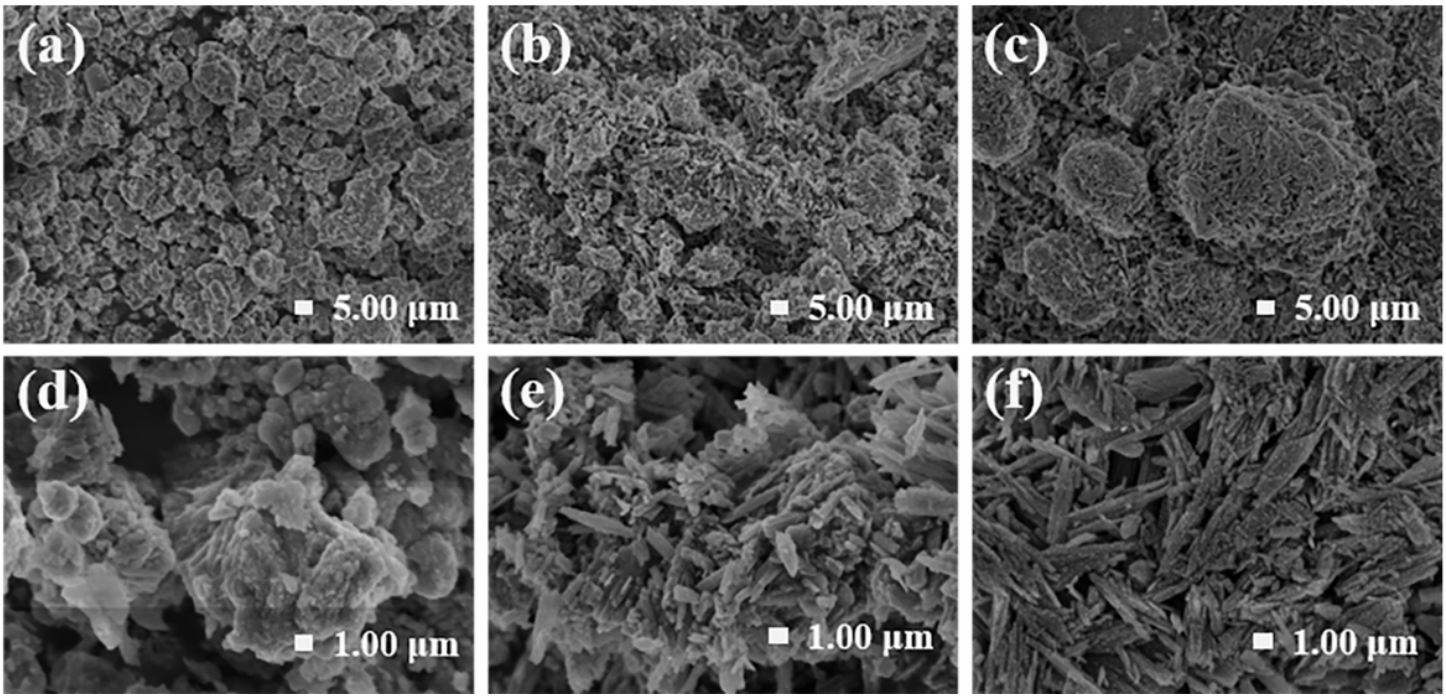

Figure 1

SEM images of each scale layer on gray cast iron pipe internal surface ((a) and (d): surface layer, (b) and (e): shell-like layer, (c) and (f) porous core layer). (d), (e), and (f) (×50 k) were the magnified images of (a), (b), and (c) (×10 k), respectively.

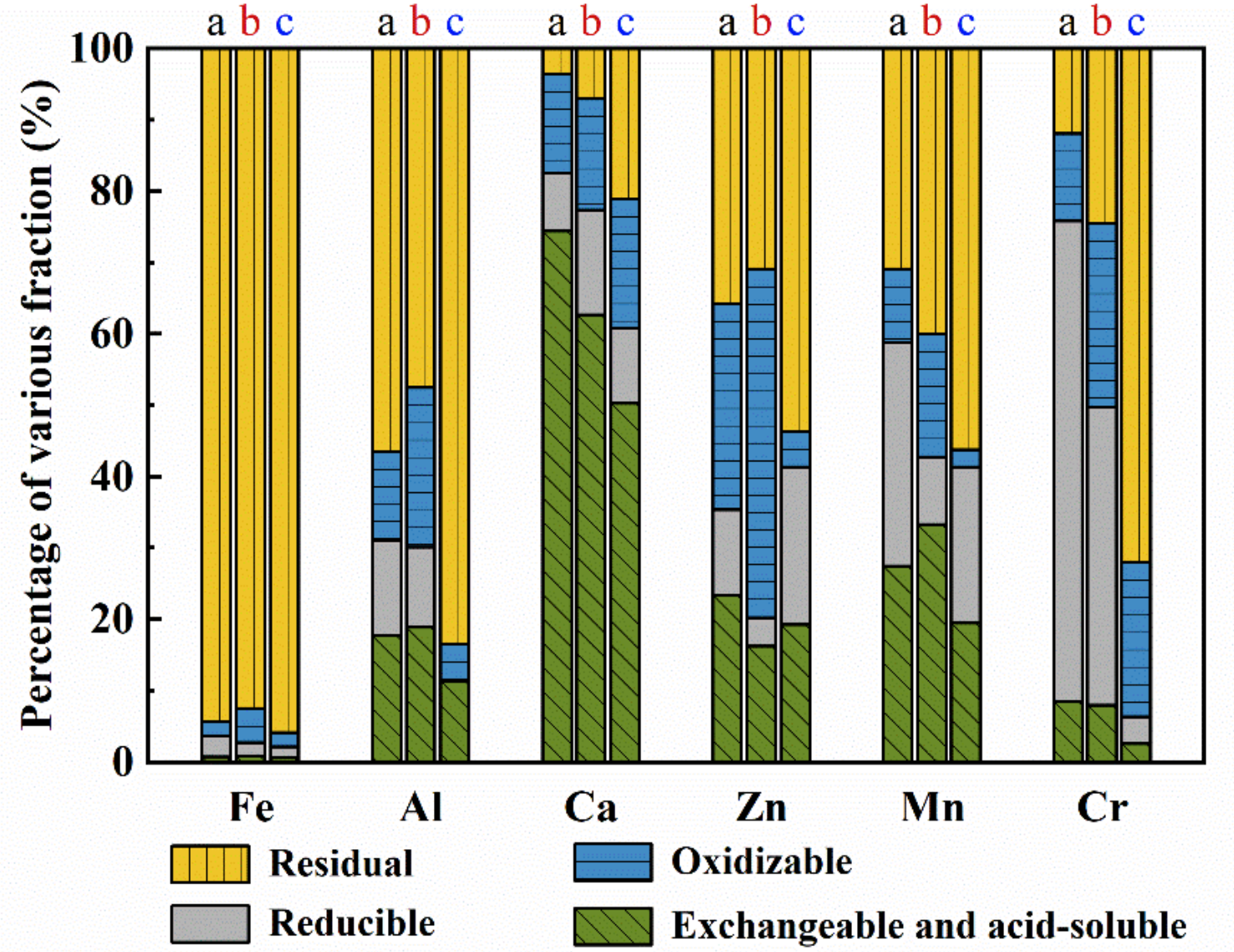

Figure 2

Speciation distributions of heavy metals in (a) surface layer, (b) shell-like layer and (c) porous core layer of corrosion scales examined by the modified BCR three-step sequential extraction method.

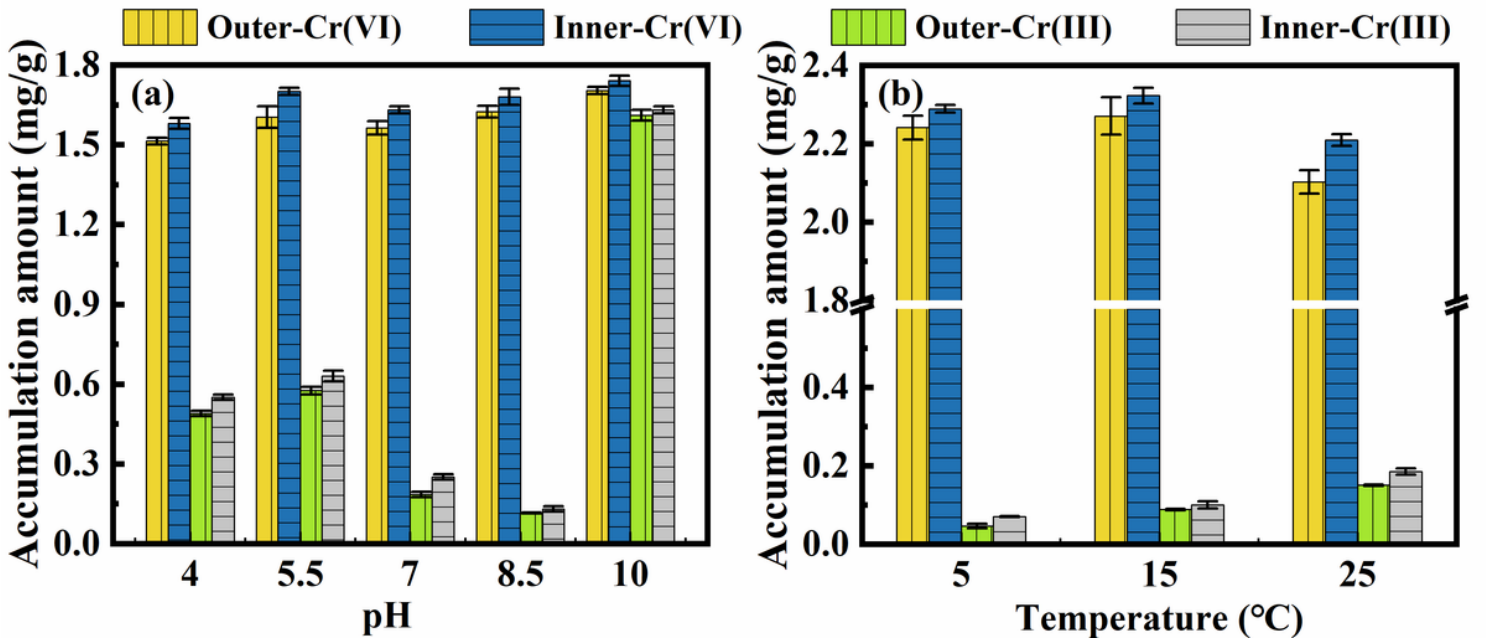

Figure 3

Effect of (a) pH and (b) temperature on Cr(VI) and Cr(III) accumulation in the outer layer and inner layer of iron corrosion scales.

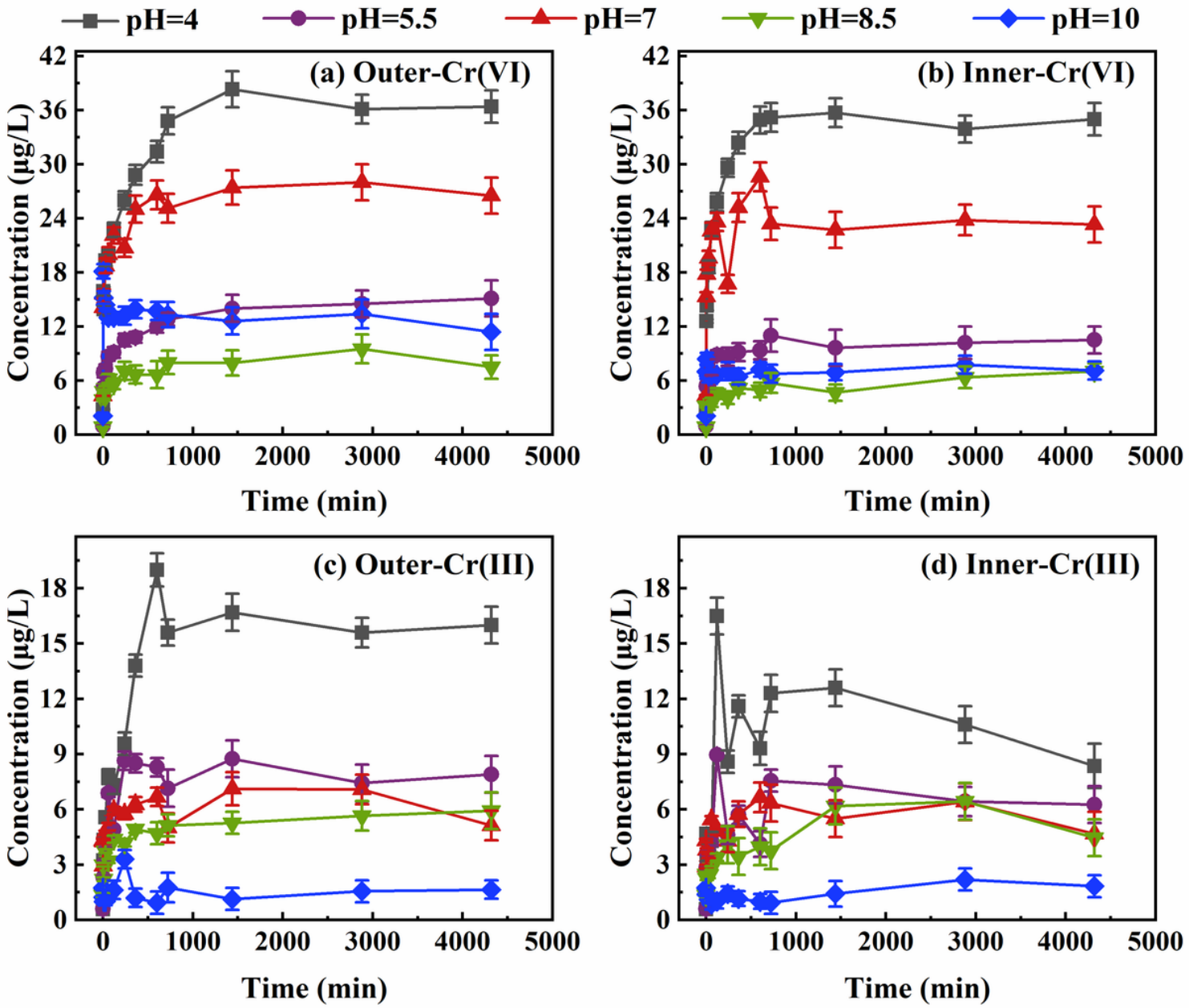

Figure 4

Effect of pH on the release of (a) outer layer Cr(VI), (b) inner layer Cr(VI), (c) outer layer Cr(III), and (d) inner layer Cr(III) from iron corrosion scales.

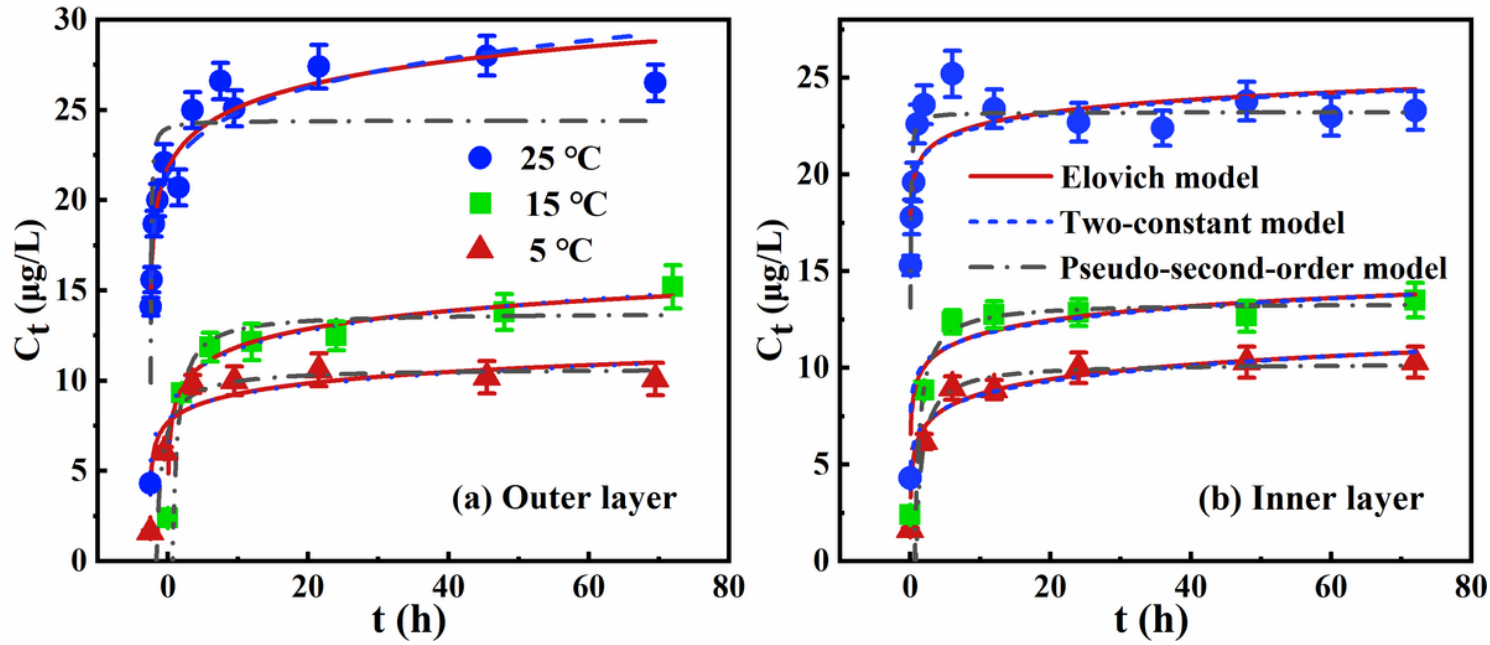

Figure 5

Data fitting using the Elovich model, Two-constant model, and Pseudo-second-order model for Cr (VI) release from the (a) outer layer, and (b) inner layer of iron corrosion scales at 25 °C, 15 °C, and 5 °C.

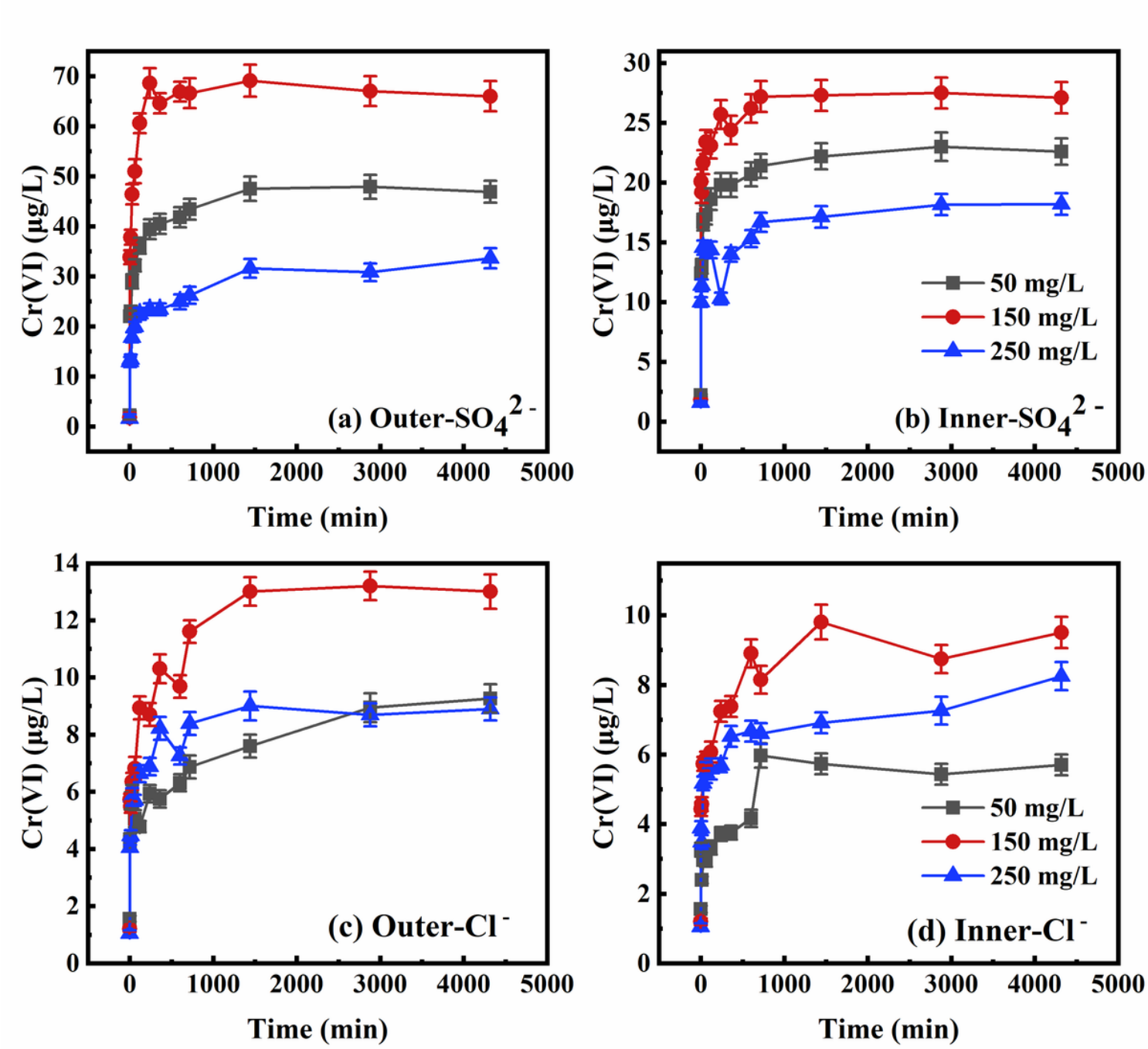

Figure 6

Effect of varying concentrations of (a) outer sulfate, (b) inner sulfate, (c) outer chloride, and (d) inner chloride on Cr(VI) release from the corresponding outer layer and inner layer of iron corrosion scales.

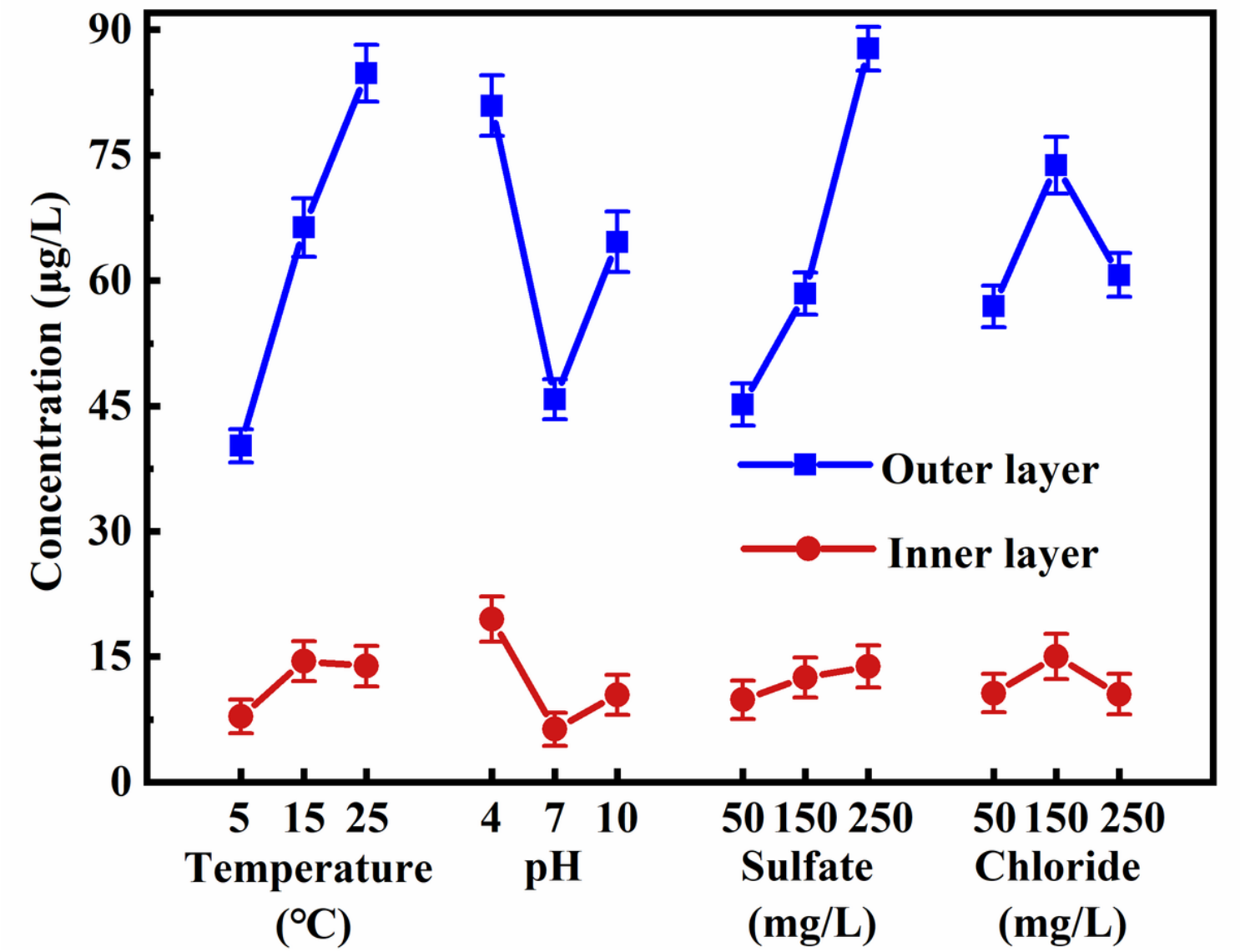

Figure 7

Range analysis for the co-effects of temperature, pH, sulfate, and chloride on Cr(VI) release from the outer layer and inner layer of iron corrosion scales.

Supplementary Files

This is a list of supplementary files associated with this preprint. Click to download.

- GraphicalAbstract.jpg
- Supplementarymaterial.docx